# Effects of particle shape and size distribution on the shear strength behavior of composite soils

**Yanrong Li**

**Abstract** The effects of particle shape and size distribution on the constitutive behavior of composite soils with a wide range of particle size were investigated. Two comparable sets of specimens were prepared: (1) mixtures of fines (clay and silt) and an ideal coarse fraction (glass sand and beads), and (2) mixtures of fines and natural coarse fraction (river sand and crushed granite gravels). Direct shear box testing was undertaken on 34 samples and the structure of the shear surfaces, change in volume and water content and the particle shape coefficient of the sheared specimens were examined. The results indicate that the contraction/dilation a specimen exhibits is restrained within the shear zone while the outer zones remain unchanged during shearing. An increased coarse fraction leads to an increase in constant volume shear strength. In addition, increasing elongation or decreasing convexity of the coarse fraction increases the constant volume friction angle. The overall roughness of the shear surface at constant volume state is negatively related to particle smoothness (convexity) and positively related to the area of the shear surface occupied by particles with particular shapes. Two equations are proposed for the estimation of constant volume friction angle based on the proportion and shape coefficient of the coarse fraction. It is hoped this will assist in considering the shear strength of mixed soils when the size of the coarse fraction makes laboratory testing difficult.

Y. Li (✉)
College of Mining Technology, Taiyuan University of Technology, Taiyuan 030024, China
e-mail: li.dennis@hotmail.com

Y. Li
AGECON Ltd., Hong Kong, China

**Résumé** Les effets de la forme et de la granularité des particules sur le comportement rhéologique de sols composites, considérant une large gamme de taille des particules, ont été étudiés. Deux ensembles comparables d'échantillons ont été préparés: (1) des mélanges de sols fins (argile et limon) avec une fraction grossière artificielle (sable de verre et perles), et (2) des mélanges de sols fins avec une fraction grossière naturelle (sable de rivière et graviers de granite concassé). Des essais de cisaillement direct à la boîte ont été réalisés sur 34 échantillons. La structure des surfaces de cisaillement, les changements de volume et de teneur en eau ainsi que le coefficient de forme des particules des échantillons cisaillés ont été analysés. Les résultats indiquent que la contractance/dilatance présentée par les échantillons ne concerne que la zone de cisaillement, tandis que les autres parties des échantillons restent inchangées pendant le cisaillement. Une augmentation de la fraction grossière conduit à une augmentation de la résistance au cisaillement à volume constant. En outre, une augmentation de l'allongement ou une diminution de la convexité des particules de la fraction grossière conduit à une augmentation de l'angle de frottement lors d'un cisaillement à volume constant. La rugosité globale de la surface de cisaillement pour un cisaillement à volume constant est reliée négativement à l'émoussé des particules (convexité) et positivement à la fraction de surface de cisaillement occupée par des particules de formes particulières. Deux équations sont proposées, pour l'estimation de l'angle de frottement relatif à un cisaillement à volume constant. Elles sont basées sur la proportion et sur le coefficient de forme de la fraction grossière. On espère que cela aidera à l'analyse de la résistance au cisaillement de

sols composites lorsque la taille de la fraction grossière rend la réalisation des essais en laboratoire difficile.

## Introduction

Understanding the effects of particle shape and size distribution on the behavior of soils helps the application and interpretation of laboratory test results (Kakou et al. 2001; Petley 1966). Since the 1950s, many investigations have considered the characteristics of various particle shape/size combinations, but the impact of different particle shape/size ratios on soil shear behaviour is still the subject of debate (Holtz and Gibbs 1956; Patwardhan et al. 1970; Vallejo and Zhou 1994; Prakasha and Chandrasekaran 2005; Cho et al. 2006).

### Influence of particle size

Holtz and Gibbs (1956) conducted triaxial tests on mixtures of gravel and sand in various proportions and concluded that the shear strength increases with gravel content greater than 50–60 % (by weight). Based on 87 large direct shear tests on sand–gravel mixtures, Simoni and Houlsby (2006) indicated that even with low gravel fractions (10–20 %), the peak strength, constant volume strength and maximum dilatancy rate of the mixtures are higher than those for pure sand at the same density. Holtz and Willard (1956) found that increasing the gravel content would increase shear resistance and decrease apparent cohesion; these investigations were based on clay with gravel contents varying from 0 to 65 %. This result was also observed by Shakoor and Cook (1990) during unconfined compressive tests on clays containing varying proportions of gravel. Patwardhan et al. (1970) presented results of direct shear tests on boulder and clay mixtures, which indicated a gradual increase in shear strength with boulder content. The same conclusion was reached by Liu et al. (2006) based on ring shear, reversal direct shear and triaxial compression tests on samples with gravel contents ranging from 0 to 40 % by weight. Miller and Sowers (1957) reported unconsolidated undrained triaxial tests on mixtures of sand and clay which showed no apparent change in friction angle but a gradual decrease of cohesion with sand content. Vallejo and Zhou (1994) reported direct shear results on mixtures of kaolinite clay and sand which indicated that the shear strength is governed by (a) the clay matrix when the sand content is less than 50 % and (b) the sand fraction when the sand content is more than 80 %. Prakasha and Chandrasekaran (2005) concluded that sand grains in clay mixtures decrease void ratio and increase friction and pore pressure response, which results in a decrease in undrained shear strength.

### Influence of particle shape

Particle shape has also been recognized as an important factor influencing the shear behavior of granular materials (Dyskin et al. 2001; Miura et al. 1998; Shimobe and Moroto 1995). Sphericity, roundness, roughness and texture are some of the terms (defined in different ways) commonly used as descriptors for particle shape (Cho et al. 2006; Santamrina and Cho 2004). Recent research revealed that increasing angularity or decreasing roundness and sphericity leads to an increase in maximum ($e_{max}$) and minimum ($e_{min}$) void ratios and the difference ($I_e$) between them (Cho et al. 2006; de Graff-Johnson et al. 1969; Santamrina and Cho 2004). Platy particles in soils lead to a decrease in packing density, stiffness and constant volume strength, while irregular particles do the opposite (Cho et al. 2006; Cubrinovski and Ishihara 2002; Guimaraes 2002; Hight et al. 1998). Holtz and Gibbs (1956) observed that angular quarry materials have much higher shear strength than subrounded and subangular river materials, based on triaxial tests on mixtures of gravel and sand. Cho et al. (2006) analyzed correlations between the particle shape and packing density, stiffness and strength of sands by employing sphericity, roundness and smoothness to describe the particle shape and surface roughness of the sands. Their study revealed that increasing irregularity causes an increase in $e_{max}$, $e_{min}$ and $I_e$; compressibility under zero-lateral strain loading; and critical state friction angle $\varphi_{cs}$, as well as a decrease in small-strain stiffness. In a previous study, the present authors (Li et al. 2013a) discussed the mechanism by which the particle shape of gravels influences the peak and constant volume friction angle of clay–gravel mixtures (40, 70 and 100 % gravel content). They concluded that an increase in asymmetry and the roughness of gravel particles increases constant volume friction angle, but tends to decrease peak friction angle.

### Composite soils

It is evident from the foregoing that

(a) both particle shape and size distribution have an influence on the shear behavior of soils,

(b) investigations into the influence of particle size distribution have mainly been focused on binary mixtures of clay–sand, sand–gravel or clay–gravel,

(c) investigations into the influence of particle shape have mainly been conducted on granular soils, e.g., sands, and

(d) experiments investigating the effects of particle shape and size distribution on the shear behavior of composite soils (characterized by a wide range of particle sizes) are rare, although composite soils are

the most frequently encountered geomaterials in engineering practice.

The present study was therefore designed to contribute to this rarely investigated causal relationship, utilizing direct shear tests on two comparable sets of samples with various proportions of particle size fractions and particle shapes. The particle sizes of the mixtures ranged up to 6.0 mm in order to represent a wide variety of soils while the normal stress varied between 200 and 400 kPa to represent the most common stress conditions encountered in practice. Volumetric change, water content and structure of shear surface or zone were analyzed.

## Testing program

### Material characteristics and sample preparation

Six types of materials were chosen as constituents for preparing the samples to be tested:

1. commercially available kaolin (particle size <2 μm),
2. non-porous soda lime glass sand (0.063–2 mm, spherical with smooth surfaces),
3. glass beads (2–6 mm, spherical with smooth surfaces),
4. naturally occurring silt (0.002–0.063 mm),
5. river sand (0.063–2 mm), and
6. gravel-size crushed granite fragments (2–6 mm).

Each constituent material was first dried in an oven at a temperature of 105 ± 0.5 °C, and then mixed and divided by the quartering method. Two sets of samples were prepared by mixing the constituent materials at the pre-specified proportions shown in Table 1. Samples in Set 1 (Samples 1–9) were mixtures of fine fraction (25 % kaolin + 75 % silt) and glass coarse fraction (50 % glass sand + 50 % glass beads), referred to as the FG mixture. Samples in Set 2 (10–17) were mixtures of fine fraction (25 % kaolin + 75 % silt) and natural coarse fraction (50 % natural sand + 50 % natural gravel), denoted as the FN mixture. Each sample was homogenized and divided into three identical specimens. Two were sheared under normal stresses of 200 and 400 kPa respectively while the third specimen was for the measurement of the moisture content of the pre-sheared specimen. As shown in Fig. 1, each sample in the FG mixture has its paired sample in the FN mixture with the same particle size distribution (e.g., Samples 2 and 10).

### Test equipment and testing procedures

It is argued that the direct shear box has some limitations, e.g., non-uniformity of stress, pre-determined location of

**Table 1** Characteristics of samples tested

| Sample no. | Fine (%) | Glass coarse (%) | Natural coarse (%) | LL (%) | PI (%) | $D_{50}$ |
|---|---|---|---|---|---|---|
| *FG mixture* | | | | | | |
| 1 | 100.0 | 0.0 | – | 45.5 | 20.1 | 0.006 |
| 2 | 80.0 | 20.0 | – | 39.2 | 21.3 | 0.008 |
| 3 | 70.0 | 30.0 | – | 35.7 | 20.2 | 0.015 |
| 4 | 60.0 | 40.0 | – | 31.4 | 18.2 | 0.025 |
| 5 | 50.0 | 50.0 | – | 24.9 | 14.3 | 0.06 |
| 6 | 40.0 | 60.0 | – | 20.8 | 11.7 | 0.2 |
| 7 | 30.0 | 70.0 | – | 16.3 | 8.9 | 0.6 |
| 8 | 20.0 | 80.0 | – | 10.1 | 4.2 | 1.0 |
| 9 | 0.0 | 100.0 | – | – | – | 2.0 |
| *FN mixture* | | | | | | |
| 10 | 80.0 | – | 20.0 | 41.6 | 22.1 | 0.008 |
| 11 | 70.0 | – | 30.0 | 37.8 | 20.1 | 0.015 |
| 12 | 60.0 | – | 40.0 | 32.1 | 16.7 | 0.025 |
| 13 | 50.0 | – | 50.0 | 26.3 | 12.7 | 0.06 |
| 14 | 40.0 | – | 60.0 | 22.9 | 11.9 | 0.2 |
| 15 | 30.0 | – | 70.0 | 17.8 | 8.6 | 0.6 |
| 16 | 20.0 | – | 80.0 | 11.4 | 4.6 | 1.0 |
| 17 | 0.0 | – | 100.0 | – | – | 2.0 |

the shear surface (Wang et al. 2007) and ambiguity in interpreting shear strength parameters at failure. However, it is still the most frequently used apparatus, especially in developing countries, due to its simple principles and the ease of testing (Salimi et al. 2008; Asmirza 2004; Cerato 2005). Potts et al. (1987) found that stresses and strains within the final failure zone are fairly uniform, and progressive failure effects were found to be minor, despite the non-uniform stresses and strains within the box before failure.

For the selection of appropriate shear box dimensions, ASTM D3080 (2004) recommends a minimum specimen width of at least 10 times the maximum particle size diameter, a minimum width to thickness ratio of 2 and a minimum initial specimen thickness of six times the maximum particle diameter. With the maximum particle size of 6.0 mm, an intermediate strain-controlled digital direct shear apparatus was used in this study (box dimensions 100 × 100 × 44 mm high). The apparatus was equipped with two digital dial gauges (readable to 2 μm) to measure vertical and shear displacements. A load cell with a measuring capacity of 4.5 kN and accuracy within ±1 % of the indicated load was utilized to measure shear force. Horizontal and vertical displacements and shear force were recorded by a data logger with a sampling frequency of 1 record per 2 μm of horizontal displacement.
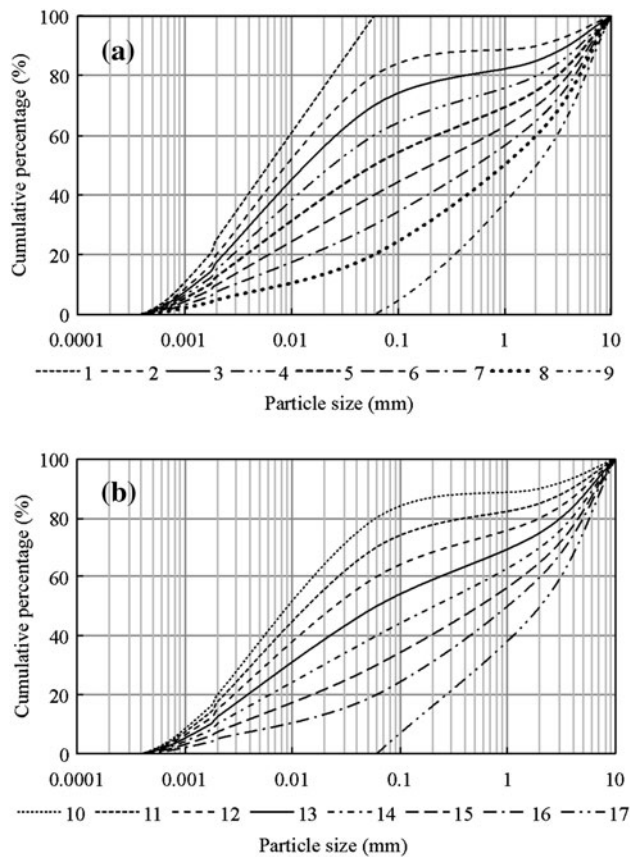
Fig. 1 Particle size distribution of the tested samples: a FG mixture and b FN mixture

For identifying the initial condition, samples with a coarse fraction of <30 % were prepared with a dry density of 1.68 Mg/m$^3$. Other samples were prepared at the same relative density of $D_r = 60$ %. The maximum and minimum void ratios were determined according to ASTM D698-07. The mixture was divided into three equal fractions. The first was carefully placed in the shear box using a spoon to prevent particle segregation and compacted using a hand rammer in order to fill one third of the shear box height. The two other layers were placed the same way.

A trial saturation test was conducted on a sample of 100 % fines which indicated the samples would be fully saturated within 36 h. Based on this, the specimens were submerged in water for 48 h prior to consolidation under the pre-specified vertical stress. Three identical specimens were prepared for each sample. After consolidation ceased, one was removed and its water content was measured (referred to as the "pre-sheared specimen"). The test conditions and results for the two "post-sheared" specimens are summarized in Table 2.

Initially, particle size distribution tests were conducted on both pre-and post-sheared samples (composed of 100 % glass coarse fraction and 100 % natural coarse fraction, respectively), to check the particle breakage/crushing

Table 2 Summary of test conditions and results

| Sample no. | Specimen no. | Testing conditions | | Constant volume state | |
|---|---|---|---|---|---|
| | | Normal stress σ (kPa) | Relative density Dr | Horizontal displacement (mm)[a] | Constant volume stress ratio $\tau_R/\sigma$ |
| 1 | 1-I | 200 | – | 7.04 | 0.41 |
| | 1-II | 400 | – | 7.81 | 0.34 |
| 2 | 2-I | 200 | – | 9.17 | 0.48 |
| | 2-II | 400 | – | 7.23 | 0.44 |
| 3 | 3-I | 200 | 0.82 | 6.94 | 0.49 |
| | 3-II | 400 | 0.82 | 6.6 | 0.45 |
| 4 | 4-I | 200 | 0.81 | 8.32 | 0.5 |
| | 4-II | 400 | 0.83 | 7.62 | 0.45 |
| 5 | 5-I | 200 | 0.82 | 5.21 | 0.49 |
| | 5-II | 400 | 0.83 | 6.12 | 0.46 |
| 6 | 6-I | 200 | 0.81 | 8.2 | 0.5 |
| | 6-II | 400 | 0.83 | 9.73 | 0.46 |
| 7 | 7-I | 200 | 0.81 | 8.32 | 0.52 |
| | 7-II | 400 | 0.82 | 8.72 | 0.47 |
| 8 | 8-I | 200 | 0.80 | 6.91 | 0.55 |
| | 8-II | 400 | 0.81 | 5.63 | 0.48 |
| 9 | 9-I | 200 | 0.81 | 5.89 | 0.59 |
| | 9-II | 400 | 0.81 | 4.72 | 0.51 |
| 10 | 10-I | 200 | 0.82 | 8.13 | 0.56 |
| | 10-II | 400 | 0.83 | 9.50 | 0.41 |
| 11 | 11-I | 200 | 0.81 | 5.37 | 0.6 |
| | 11-II | 400 | 0.83 | 6.55 | 0.52 |
| 12 | 12-I | 200 | 0.82 | 7.85 | 0.64 |
| | 12-II | 400 | 0.81 | 8.04 | 0.62 |
| 13 | 13-I | 200 | 0.81 | 9.01 | 0.67 |
| | 13-II | 400 | 0.81 | 7.13 | 0.63 |
| 14 | 14-I | 200 | 0.80 | 8.8 | 0.69 |
| | 14-II | 400 | 0.81 | 6.47 | 0.65 |
| 15 | 15-I | 200 | 0.81 | 4.97 | 0.72 |
| | 15-II | 400 | 0.81 | 7.27 | 0.72 |
| 16 | 16-I | 200 | 0.80 | 7.09 | 0.94 |
| | 16-II | 400 | 0.81 | 6.29 | 0.76 |
| 17 | 17-I | 200 | 0.80 | 8.03 | 0.97 |
| | 17-II | 400 | 0.80 | 7.39 | 0.89 |

[a] Horizontal displacement at which the constant volume state reached

during direct shear tests at a normal stress of 400 kPa. No particle breakage was found for samples composed of glass coarse fraction. However, some crushing was recorded in the natural coarse particles, this was considered negligible (the coarse fraction decreasing by <0.4 %). To allow complete drainage, all tests were conducted at a low shearing rate of 0.006 mm/min according to ASTM D3080 (2004) for a sufficient time to achieve consolidation and possible horizontal displacement to reach failure.
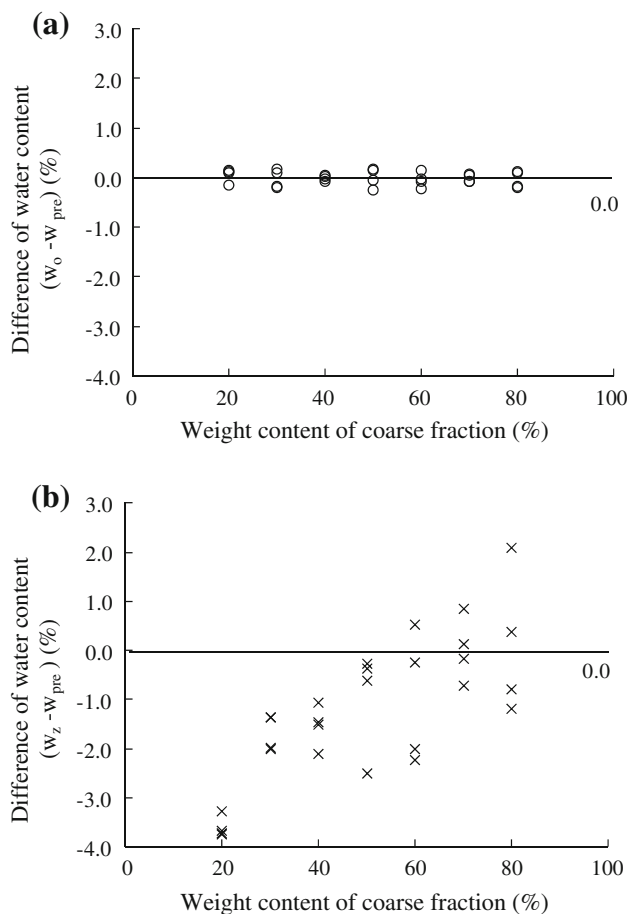
Fig. 2 Difference in water content: **a** between pre-sheared specimen and outer zone of post-sheared specimen, and **b** between pre-sheared specimen and shear zone of post-sheared specimen

## Results

### Pre- and post-sheared water contents

The water contents of the pre- and post-sheared specimens were determined immediately after removal from the sample chamber and wiping off any free water on the surfaces. Then, pieces of samples were cut from the top, middle and bottom layers of the specimens. The water contents of the three pieces of the pre-sheared specimen were found to be almost the same with a standard deviation of less than 0.1 %; the average value was used as the water content of the pre-sheared specimen ($w_{pre}$). For the post-sheared specimen, a strip was cut from the middle of the sheared sample and its water content was taken to represent the shear zone ($w_z$). By considering the ratio (5:10) of shear zone thickness to mean particle size $d_{50}$, as reported by previous researchers (Roscoe 1970; Bridgwater 1980; Hartley 1982; Scarpelli and Wood 1982; Dejong et al. 2003), the thickness of the strip sample varied from 5 mm (for samples with 0 % coarse fraction) to 10 mm (80 % coarse fraction). The water content of the

upper and lower zones ($w_o$) was determined on the 40 g specimen from the top and bottom layers. The water contents of Samples 9 and 17 were not measured as these samples were composed of only coarse fraction and hence free draining.

The differences in water contents for the pre-sheared and top and bottom layers of post-sheared specimens are plotted in Fig. 2a which indicates only minor deviations (<0.3 %) and suggests that shearing did not introduce much change in the water content of the outer zones compared with the pre-sheared specimen. However, as shown in Fig. 2b, the differences in water contents between the shear zone ($w_z$) and pre-sheared specimen ($w_{pre}$) reached as much as 3.8 %. Furthermore, this difference showed a strong dependency on the weight percentage of the coarse fraction. As the specimens were kept submerged during shearing, they were assumed to remain fully saturated; the shearing rate employed was slow to allow full drainage. Thus comparison of water content profile across a post-sheared specimen with that of a pre-sheared specimen should reflect shear-induced structure deviation.

### Shear surface structure

After removal from the shear box, each sheared specimen was split along its shear surface. As shown in Fig. 3, the slickensides gradually disappear and the shear surfaces become rougher with increasing coarse fraction in the FG mixtures.

(a)  The shear surface of Specimen 1-I (no coarse fraction) is poorly polished, even and slickensided in the direction of shear;

(b)  The shear surface of Specimen 3-I (30 % glass coarse fraction) is characterized by some discontinuous slickensides interrupted by coarse particles;

(c)  Specimen 5-I (50 % coarse fraction) has a few local slickensides and a local accumulation of coarse particles with surrounding fines.

In the case of FN mixtures the shear surface gets rougher and more porous with increasing coarse fraction.

(a)  The shear surface of Specimen 10-I (20 % natural coarse fraction) has a relatively flat surface and discontinuous slickensides, poorly developed and disrupted by coarse particles;

(b)  Specimen 11-I (30 % coarse fraction) exhibits weak and short slickensides scattered over the surface;

(c)  Specimen 13-I (50 % coarse fraction) shows no obvious evidence of slickensides but a shear zone resembling a reworked soil mass with an identifiable shear-induced structure.

Based on these observations, two inferences can be made: (1) increasing coarse fraction deters the development of
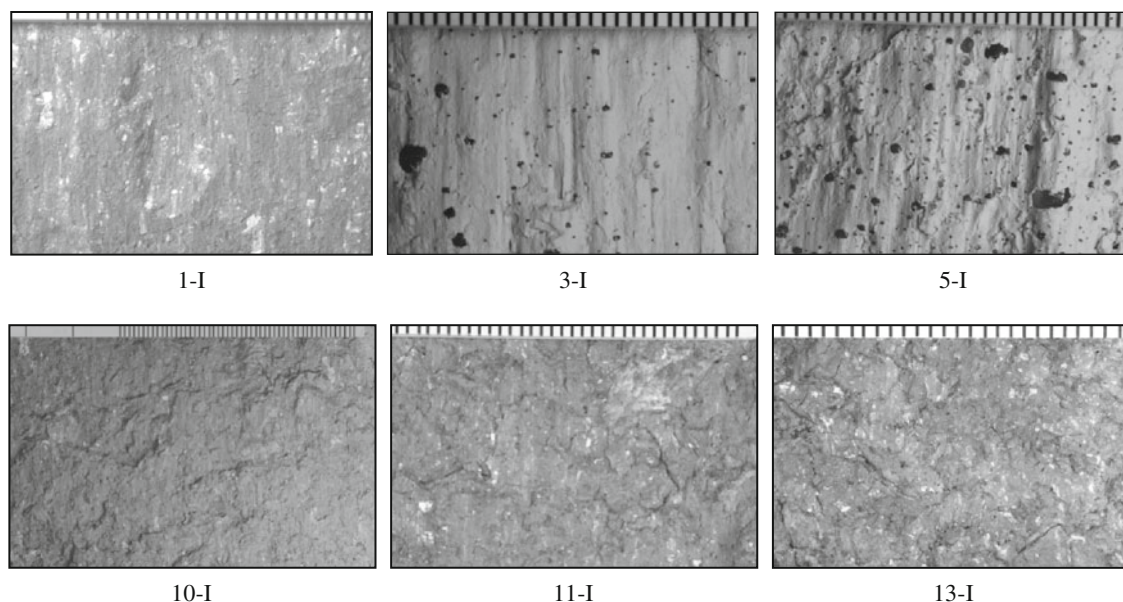
Fig. 3 Photos of the shear surfaces of specimens tested

slickensides and produces rougher and more uneven shear surfaces, and (2) an FN mixture produces rougher and more porous shear surfaces than an FG mixture with the same particle size distribution (e.g., Samples 3 and 11).

Shape coefficient of tested samples

Two parameters, convexity and elongation, derived from 2D images of the soil particles were used to quantify the particle shape. As shown in Fig. 4, "convexity" measures surface roughness given by the ratio of "convex hull perimeter" to the actual particle perimeter and is not affected by the overall form. It ranges from 1.0 for a smooth particle to zero for a very irregular one. "Elongation" is a measure of particle symmetry and equals "1.0-aspect ratio" or "1.0-width/length". It is unaffected by surface roughness. A particle symmetrical in all axes, such as a circle, would have an elongation value of zero, whereas particles with small aspect ratios have an elongation close to 1.0. The image capture and analysis were conducted with a stereo-microscope (Olympus SZH10) equipped with the image process program AnalySIS®.

The glass sand and beads in the FG mixtures are perfectly spherical and smooth, with a convexity of 1.0 and an elongation of 0.0. The particle shape parameters for silt, river sand and crushed granite gravels were determined from the stereo-microscope images (Fig. 5a, b, c), and the parameters for the kaolin particles were determined from images taken by a scanning electron microscope (Fig. 5d). The number of randomly selected particles from each particle size fraction was normally hundreds to a thousand and the statistical standard deviation of each parameter was

less than 0.04. Values of particle shape parameters for the constituent materials are listed in Table 3.

In the statistical sense, it is not the weight percentage but the area ratio (the ratio of area occupied by a constituent material to the total area of the shear surface) that directly influences the development of a shear surface and the mode of shear. In this study, the shape parameters for the fine fraction (25 % clay + 75 % silt), coarse fraction (50 % sand + 50 % gravel) and each tested sample were calculated as the weighted sum of the mean shape parameter values for each constituent material (i.e., scaled by its area/volume ratio $\upsilon$ in the mixture). The volume ratio of each constituent material was calculated as:

$$\upsilon = \frac{volume\ of\ each\ constituent\ material}{sum\ of\ volume\ of\ constituent\ materials} = \frac{\frac{M}{R}}{\sum \frac{M}{R}} \quad (1)$$

where M = dry mass of constituent material in a specimen, and R = particle density of constituent material. The value so obtained for statistically quantifying particle shape of the fine and coarse fractions and the soil mixture is defined as the 'shape coefficient' in order to avoid confusion with the 'shape parameter' of the individual particles.

## Discussion

### Volumetric change

As explained above, assuming the specimens remained fully saturated during shearing, changes in water contents reflect changes in their void ratio. The minimal difference between the water contents of the unsheared specimens and

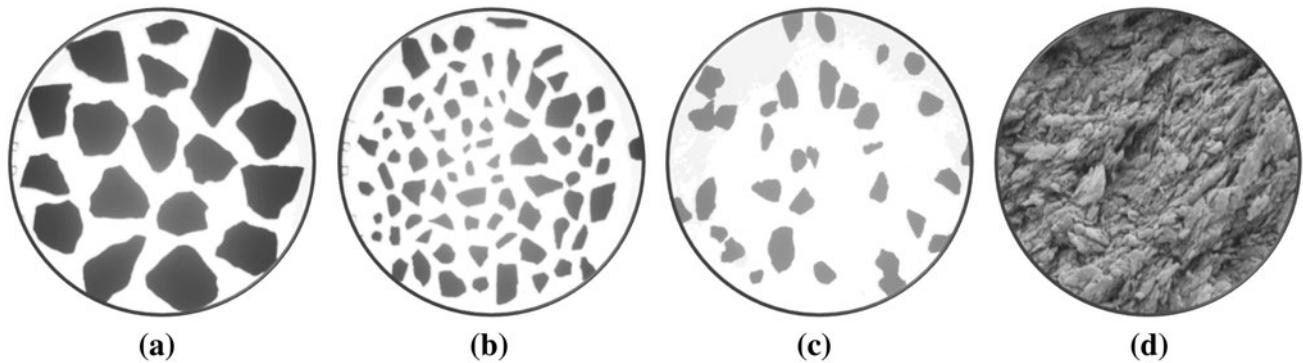| | ● | ▬ | ■ | ▬ | ✹ | ✦ |
|---|---|---|---|---|---|---|
| Circularity | 1 | 0.47 | 0.89 | 0.52 | 0.47 | 0.21 |
| Convexity | 1 | 1 | 1 | 1 | 0.70 | 0.73 |
| Elongation | 0 | 0.82 | 0 | 0.79 | 0.24 | 0.83 |

Fig. 4 Illustration of particle shape parameters (Malvern 1999)



Fig. 5 Microscopic images of particles: a gravel, b sand, c silt, and d kaolin, for determination of particle shape parameters

the top and bottom layers of the sheared specimens (Fig. 2a) indicates the shearing did not influence void ratio in the outer zones. However, the water contents of unsheared specimens and shear zones of sheared specimens displayed strong negative and positive differences (Fig. 2b) suggesting a reduced void ratio attributed to densification/contraction (negative) and increased void ratio due to loosening/dilation (positive) within the shear zone. As shown in Fig. 6, the relationship between vertical displacements ($\gamma$) at constant volume state and the water content differences ($\delta$) can be expressed by

$$\gamma = 0.144\delta \quad (R^2 = 0.78) \tag{2}$$

The zero intercept in Eq. 2 implies that no volumetric change would occur if there was no change in water content of the shear zone. These observations confirm that volumetric dilation and contraction in sheared specimens mainly reflect changes in void structure of their shear zones. Li et al. (2013b) drew the same conclusion for binary mixtures of kaolin and glass beads. These inferences are also in agreement with Tatsuoka et al. (1990), Mitchell (1993) and Wu et al. (2008) who, based on investigations of shear bands in granular materials, concluded that disturbance of the shear zone accounts for the bulk of the observed volume changes.

Figures 2 and 6 also strongly suggest that increasing coarse fraction promotes shear zone dilation, while reducing it favors volumetric contraction associated with the re-organization of the soil fabric in the shear zone.

When a sample with little or no coarse fraction (e.g., Sample 1) is sheared, a well slickensided shear surface (Fig. 3) develops with fine particles aligned in the direction parallel to shearing. The reorientation of the fine particles causes a volumetric contraction and a denser shear zone (de Graff-Johnson et al. 1969). On the other hand, when a sample with a large coarse fraction (e.g., Sample 5) is sheared, the constant volume state is reached at maintained volumetric dilation due to interlocking of coarse particles (Li and Aydin 2010; Taylor 1948). In such samples, the shear zone is normally looser than the outer zones and contains more water (Fig. 6). This is in good agreement with the findings by Oda and Konishi (1974), Fukuoka et al. (2006), Li and Aydin (2010) and Li et al. (2012) that dense granular materials reach their constant volume state when a looser shear zone develops, within which large particles tend to rotate or roll, minimizing resistance to movement.

Constant volume shear strength

Table 2 summarizes the test results in terms of constant volume stress ratio and the shear displacement at which the constant volume state is reached. Figure 7 gives sample plots showing the development of stress ratio and volumetric dilation with shear displacement. The tested specimens reached constant volume state at a horizontal displacements ranging from 4.5 to 9.5 mm, although no obvious relationship between this displacement and

**Table 3** Particle shape parameters of the tested materials

| Material | Convexity | Elongation |
|---|---|---|
| Glass sand | 1.00 | 0.00 |
| Glass bead | 1.00 | 0.00 |
| River sand | 0.81 | 0.30 |
| Crushed granite gravel | 0.56 | 0.70 |
| Silt | 0.75 | 0.28 |
| Kaolin | 0.84 | 0.30 |
| Fine fraction | 0.77 | 0.29 |
| Glass coarse fraction | 1.00 | 0.00 |
| Natural coarse fraction | 0.69 | 0.50 |
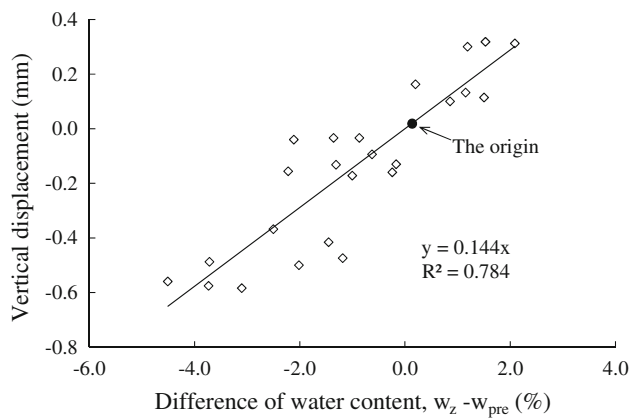


**Fig. 6** Difference in water content between pre-sheared specimen $w_{pre}$ and shear zone of post-sheared specimen $w_z$ as a function of vertical displacement at constant volume state

particle size distribution or particle shape parameters was observed. Area correction for shear stress was conducted as recommended by Xu et al. (2007) and Li et al. (2013b). The constant volume friction angle $\varphi_{cv}$ was derived from $\varphi_{cv} = \tan^{-1}(\tau_{cv}/\sigma)$, where $\sigma$ is normal stress and $\tau_{cv}$ is shear stress at constant volume state.

The constant volume (residual) friction angle $\varphi_{cv}$ is plotted in Fig. 8 versus weight percent of the coarse fraction. The $\varphi_{cv}$ values of the specimens composed of (a) 100 % fine fraction (b) 100 % glass coarse fraction and (c) 100 % natural coarse fraction were approximately 20°, 30° and 44° respectively. These values are within the ranges obtained by Cerato (2005), Yagiz (2001), Yazdanjou (2008) and Salimi et al. (2008) from direct shear tests on similar soil mixtures. The increase in $\varphi_{cv}$ values with coarse fraction may be attributed to the increased contact and interactions between the coarse particles. As illustrated in Fig. 3, the mixture with a high proportion of fine fraction developed slickensided shear surfaces and behaved dominantly in the sliding mode with low constant volume shear strength. With an increase in coarse fraction, the shear
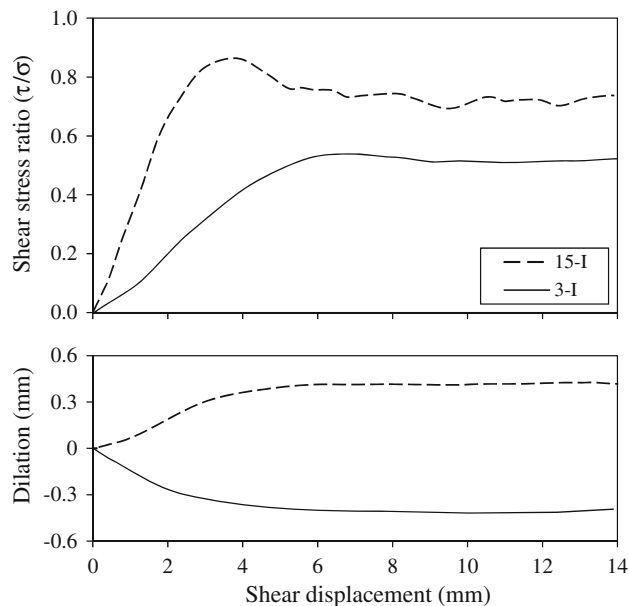


**Fig. 7** Plots of shear stress ratio ($\tau/\sigma$) and vertical displacement against shear displacement for Specimens 3-I and 15-I

surface becomes rougher; the coarse particles having a higher friction than clay particles.

Figure 8 also reveals that the constant volume shear strength was normal stress-dependent as $\varphi_{cv}$ values of specimens sheared at 200 kPa were greater than those sheared at 400 kPa. This dependency existed in both FG and FN mixtures. Stark and Eid (1994) and Li et al. (2013b) discussed this dependency and argued that a high normal stress favours face-to-face interactions of platy particles, leading to a relatively smooth shear surface and a low constant volume friction angle in soils with high fine fraction. Based on the images of shear surfaces, Li et al. (2013b) argued that in mixed soils with high normal stresses, the coarse particles are pushed into the fine matrix, such that there is a dominance of fines in the zone of shear, lowering $\varphi_{cv}$. Other notable observations from Fig. 8 include

1. FN mixture has higher $\varphi_{cv}$ than FG mixture with the same coarse fraction (where the difference can be as much as 18° between Samples 9 and 17), and
2. This increasing pattern of $\varphi_{cv}$ is of divergence and cannot be fitted by a regression function taking the coarse fraction as the only independent variable.

These issues are discussed in the following sections by taking into account the shape coefficient.

Shape coefficient of coarse fraction

The constant volume friction angle $\varphi_{cv}$ is plotted in Fig. 9 against shape coefficient of coarse fraction calculated with Eq. 1. Only specimens sheared under 200 kPa are shown
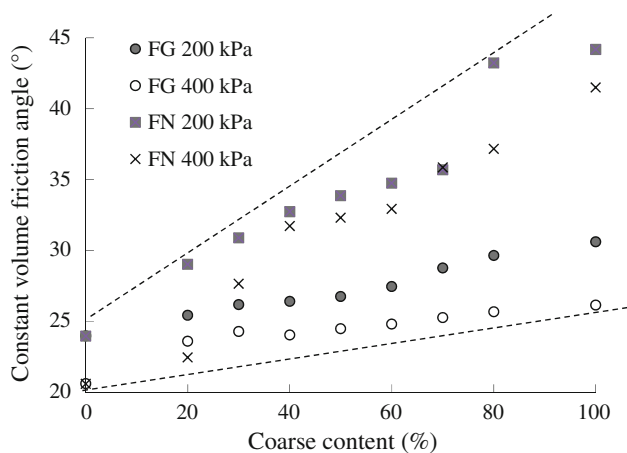
Fig. 8 Constant volume friction angle increases with weight content of coarse fraction
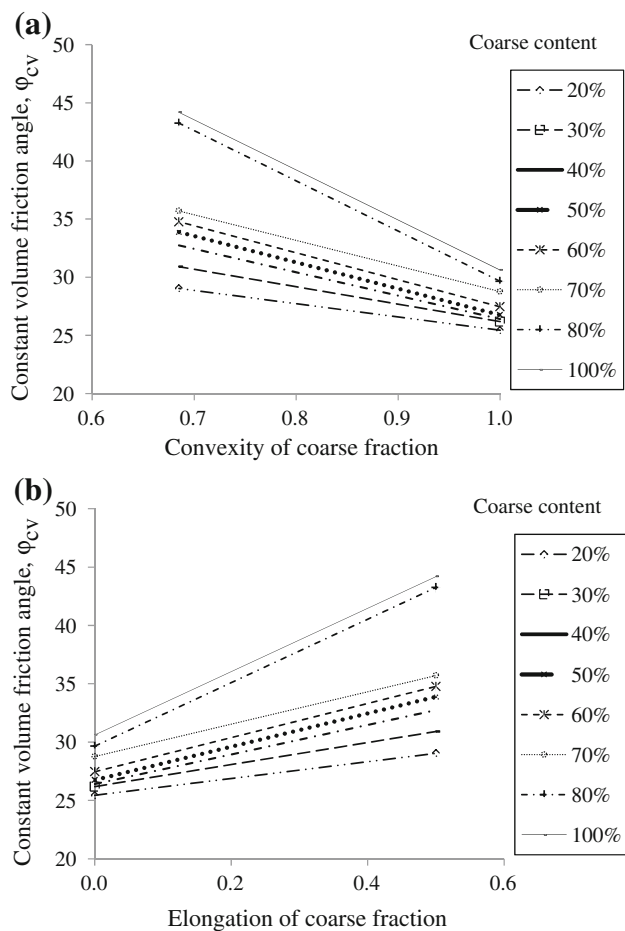


Fig. 9 Relationship between constant volume friction angle $\varphi_{cv}$ and shape coefficients of coarse fraction: **a** convexity, and **b** elongation

for clarity. It can be observed that the $\varphi_{cv}$ value decreases with convexity of coarse fraction (Fig. 9a), and it increases with elongation (Fig. 9b), regardless of the content of

coarse fraction. The $\varphi_{cv}$ value of FG mixtures ranges from 20° to 30° and that of FN mixtures from 20° to 45° (Figs. 8, 9). Substituting glass coarse fraction by natural coarse fraction resulted in an increase of 3° for mixtures with 20 % coarse fraction (Samples 2 and 10) and up to 18° for mixtures with 100 % coarse fraction (Samples 9 and 17). Agreeing with this, FG samples developed obvious slickensided shear surfaces, while FN samples exhibited rough and uneven shear surfaces, as shown in Fig. 3.

The constant volume friction angle $\varphi_{cv}$ of a shear surface is governed by its overall roughness. The roughness is in turn determined by the area occupied by soil fractions with different particle size, shape and friction characteristics. As asymmetric (elongated) particles (prismatic or disk shaped) have a greater surface area than symmetrical ones (rounded or spherical), the shear surface area occupied by the natural coarse fraction in FN mixtures (e.g., Sample 3) is expected to be statistically greater than that occupied by the glass coarse fraction in FG mixtures (e.g., Sample 11). In addition, the friction between natural coarse particles (convexity = 0.69) is greater than that between the glass particles (convexity = 1.0) hence the shear surfaces in the FN mixtures are rougher and have a higher $\varphi_{cv}$ than those in FG mixtures.

Multi-variable regression analysis was conducted by taking $\varphi_{cv}$ as the dependent variable and content (CF), convexity (CON) and elongation (EL) of the coarse fraction as independent variables, in order to establish a model combining the relationships revealed in Figs. 8 and 9. Coarse fraction content was expressed as a decimal in order to be within the same scale range (0–1.0) as convexity and elongation. The analysis yielded the following equation:

$$\varphi_{cv} = 12.7CF - 2.0CON + 13.2EL + 23.1 \quad (R^2 = 0.88) \tag{3}$$

The regression coefficients in Eq. 3 indicate that for the coarse fraction, both content and elongation have a strong positive influence on the $\varphi_{cv}$ value, while convexity has a relatively small negative effect.

Another strong multivariable relationship was found to predict the difference between the $\varphi_{cv}$ values of any specimen of a given mixture and that of the specimen composed of pure fine fraction of the same mixture ($\Delta\varphi_{cv}$):

$$\Delta\varphi_{cv} = 220\delta_{EL} + 300\delta_{CON} \quad (R^2 = 0.97) \tag{4}$$

where $\delta_{EL}$ and $\delta_{CON}$ are differences in the elongation and convexity coefficients, respectively, of the two specimens. For example, there is $\Delta\varphi_{cv} = \varphi_{cv(2\text{-I})} - \varphi_{cv(1\text{-I})}$ between Specimen 2-I and Specimen 1-I.

Equation 3 provides a means of estimating the constant volume shear strength of soils with fine and coarse fractions in terms of the coarse fraction content, as well as the

convexity and the elongation of the coarse fraction. The latter parameter is easily measured or estimated by comparing the soil particles with the standard particle shape charts as in Fig. 4. Equation 4 can be used as a reference or an independent means of estimating $\varphi_{cv}$ of a soil if the $\varphi_{cv}$ of its fine fraction is known or can be estimated. Due to the small size of the test apparatus used in practice, discarding the coarse fraction and testing only the fine fraction of a soil is the common approach. The test results so obtained, generally underestimate the actual strength of soils represented by their complete particle size distribution. It was confirmed in this study, that the constant volume friction angle increases with coarse fraction. Hence, Eq. 4 may be employed to evaluate the actual strength of a soil, based on the strength of its fine fraction.

## Conclusions

Two types of specimen were prepared, with varying proportions of an artificial or a natural coarse fraction (FG and FN). These were tested in a direct shear box to explore the effects of varying particle shape and size distributions on the constant volume shear strength of well-graded soil mixtures up to a maximum particle size of 6 mm.

The study involved determining the water content of unsheared and sheared specimens, examining the shear surface structures and deriving relationships between constant volume friction angle and particle shape coefficients. The results indicated that samples having a high proportion of fine fraction experience volumetric contraction due to particle alignment and densification, which in turn lowers the water content within the shear zone. A slickensided shear surface develops in such soils, reducing the constant volume friction angle. By contrast, samples with a high proportion of coarse fraction experience shear zone dilation due to particle interlocking, a looser shear zone with an increased water content relative to the unsheared specimens. The study has shown that the change in structural characteristic of the shear zone is responsible for the volumetric change of the tested specimens.

Increasing the coarse fraction increases the constant volume friction angle of the soil mixtures. This response can be exacerbated by changing the particle shape; increasing elongation or decreasing convexity increases the constant volume friction angle.

The results also indicate that the overall roughness of the shear surface, at constant volume state, is negatively related to particle smoothness (convexity) whilst positively related to the area of the shear surface.

From this study, two equations were obtained, enabling estimation of the constant volume friction angle based on the proportion and shape coefficient of the coarse fraction.

Therefore, these equations may be used as an aid to estimate shear strength where the size of the coarse fraction makes testing problematic.

## References

American Society for Testing and Materials (2004) ASTM D3080—04 Standard Test Method for Direct Shear Test of Soils Under Consolidated Drained Conditions

Asmirza FT (2004) Direct shear testing. Technical Report, University of Sumatera Utara

Bridgwater J (1980) On the width of failure zones. Geotechnique 30(4):533–536

Cerato AB (2005) Scale effects of shallow foundation bearing capacity on granular materials. PhD dissertation, University of Massachusetts, Amberst

Cho GC, Dodds J, Santamarina JC (2006) Particle shape effects on packing density, stiffness, and strength: natural and crushed sands. J Geotech Geoenviron Eng 132:591–602

Cubrinovski M, Ishihara K (2002) Maximum and minimum void ratio characteristics of sands. Soils Found 42(6):65–78

de Graff-Johnson JWS, Bhatia HS, Gidigasu DM (1969) The strength characteristics of residual micaceous soils and their application to stability problems. In: Proc. 7th Int'l Conf Soil Mech Found Engrg Mexico, pp 165–172

Dejong JT, Randolph ME, White DJ (2003) Interface load transfer degradation during cyclic loading: a micro-scale investigation. Soils Found 43(4):81–93

Dyskin AV, Estrin Y, Kanel-Belov AJ, Pasternak E (2001) Toughening by fragmentation—how topology helps. Adv Eng Mater 3(1):885–888

Fukuoka H, Sassa K, Wang G, Sasaki R (2006) Observation of shear zone development in ring-shear apparatus with a transparent shear box. Landslides 3(2):239–251

Guimaraes M (2002) Crushed stone fines and ion removal from clay slurries—fundamental studies. Ph.D. thesis, Georgia Institute of Technology, Atlanta

Hartley S (1982) Shear bands in sand, Part II. Project report, Department of Engineering, University of Cambridge

Hight DW, Georgiannou VN, Martin PL, Mundegar AK (1998) Flow slides in micaceous sand. In: Yanagisawa E, Moroto N, Mitachi T (eds) Problematic soils. Sendai, Japan, pp 945–958

Holtz WG, Gibbs HJ (1956) Triaxial shear tests on previous gravelly soils. J Soil Mech Found Div ASCE 820(SM1):1–22

Holtz WG, Willard M (1956) Triaxial shear characteristics of clayey gravel soils. J Soil Mech Found Eng ASCE 82:143–149

Kakou BG, Shimizu H, Nishimura S (2001) Residual strength of colluvium and stability analysis of farmland slope. Agric Eng Int CIGR J Sci Res Dev 3:1–12

Li YR, Aydin A (2010) Behavior of rounded granular materials in direct shear: mechanisms and quantification of fluctuations. Eng Geol 115(1–2):96–104

Li YR, Huang RQ, Chan LS, Chen J (2013a) Effects of particle shape on shear strength of clay-gravel mixture. J Civil Eng KSCE 17(4):712–717

Li YR, Chan LS, Yeung AT, Xiang XQ (2013b) Effects of test conditions on shear behavior of composite soil. Geotech Eng Proc ICE 166(3):310–320

Li YR, Aydin A, Xu Q, Chen J (2012) Constitutive behavior of binary mixtures of kaolin and glass beads in direct shear. J Civil Eng KSCE 16(7):1152–1159

Liu XL, Loo H, Min H, Deng JH, Tham LG, Lee CF (2006) Shear strength of slip soils containing coarse particles of Xietan landslide. In: Proceedings of sessions of Geo Shanghai, pp 195–207

Malvern Instruments (1999) Image analysis application note. Available at www.malvern.com/particleshape

Miller EA, Sowers GF (1957) The strength characteristics of soil-aggregate mixture. Highw Res Board Bull 183:16–23

Mitchell JK (1993) Fundamentals of soil behavior, 2nd edn. Wiley

Miura K, Maeda K, Furukawa M, Toki S (1998) Mechanical characteristics of sands with different primary properties. Soils Found 38:159–172

Oda M, Konishi J (1974) Microscopic deformation mechanism of granular material in simple shear. Jpn Soc Soil Mech Found Eng 14(4):25–38

Patwardhan AS, Rao JS, Gaidhane RB (1970) Interlocking effects and shearing resistance of boulders and large size particles in a matrix of fines on the basis of large scale direct shear tests. In: Proc 2nd Southea Asian conf soil mech Singapore, pp 265–273

Petley DJ (1966) The shear strength of soils at large strains. PhD thesis, University of London

Potts DM, Dounias GT, Vaughan PR (1987) Finite element analysis of the direct shear box test. Geotechnique 37(1):11–23

Prakasha KS, Chandrasekaran VS (2005) Behavior of marine sand–clay mixtures under static and cyclic triaxial shear. J Geotech Geoenviron Eng 131(2):213–222

Roscoe KH (1970) Tenth rankin lecture: the influence of strains in soil mechanics. Geotechnique 20(2):129–170

Salimi SN, Yazdanjou V, Hamidi A (2008) Shape and size effects of gravel grains on the shear behavior of sandy soils. In: Chen (eds) Proceedings of 10th intl' conf. on landslides and engineered slopes. China, pp 469–474

Santamrina JC, Cho GC (2004) Soil behavior: the role of particle shape. In: RJJardine, DMPotts, KG Higgins (Eds) Advances in geotechnical engineering: the skempton conference, vol 1. Thomas Telford, London, 604–617

Scarpelli G, Wood DM (1982) Experimental observations of shear band patterns in direct shear tests. In: IUTAM conference on deformation and failure of granular materials

Shakoor A, Cook BD (1990) The effect of stone content, size and shape on the engineering properties of a compacted silty clay. Bull Assoc Eng Geol XXVII(2): 245-253

Shimobe S, Moroto N (1995) A new classification chart for sand liquefaction. In: Ishihara K (ed) Earthquake geotechnical engineering. Balkema, Rotterdam, pp 315–320

Simoni A, Houlsby GT (2006) The direct shear strength and dilatancy of sand–gravel mixtures. Geotech Geol Eng 24:523–549

Stark TD, Eid HT (1994) Drained residual strength of cohesive soils. J Eng ASCE 120(5):856–871

Tatsuoka F, Nakamura S, Huang CC, Tani K (1990) Strength anisotropy and shear band direction in plane strain tests of sand. Soils Found 30(1):35–56

Taylor DW (1948) Fundamentals of soil mechanics. Wiley, New York

Vallejo LE, Zhou Y (1994) The mechanical properties of simulated soil-rock mixtures. In: Proc 13th int'l conf soil mech and found engrg, New Delhi, pp 365–368

Wang J, Dove JE, Gutierrez MS (2007) Discrete-continuum analysis of shear banding in the direct shear test. Geotechnique 57(6):513–526

Wu PK, Matsushima K, Tatsuoka F (2008) Effects of specimen size and some other factors on the strength and deformation of granular soil in direct shear tests. Geotech Test J 31(1):1–20

Xu Z, Zhou G, Liu Z, Zhou J, Tian Q (2007) Correcting method and error analysis for sample area in direct shear test. J China Univ Min Tech 36(5):658–662

Li YR, Huang RQ, Chan LS (accepted for publication) The rule of particle shape in shear strength of clay-gravel mixture. J Civil Eng KSCE

Yagiz S (2001) Brief note on the influence of shape and percentage of gravel on the shear strength of sand and gravel mixtures. Bull Eng Geol Environ 60(321):323

Yazdanjou, V, Salimi N, Hamidi A (2008) Effect of gravel content on the shear behavior of sandy soils. In: Proc. 4th national cong. on civil engrg, Tehran University, Iran